Journal of Advanced Marine Engineering and Technology, Vol. 49, No. 6, pp. 489~495, 2025
J. Advanced Marine Engineering and Technology (JAMET)
https://doi.org/10.5916/jamet.2025.49.6.489

ISSN 2234-7925 (Print)
ISSN 2765-4796 (Online)
Original Paper

Corrosion behavior analysis of high-corrosion-resistant Zn-flake coatings

Yeonwon Kim[1] · Kyunghwang Lee[2] · Jeonghyeon Yang†

(Received December 10, 2025 ; Revised December 19, 2025 ; Accepted December 23, 2025)

Abstract: The corrosion behavior of a Zn-flake coating—consisting of a Zn-flake topcoat and a high-corrosion-resistant Zn-based base layer—was comprehensively evaluated in comparison with electro-galvanized (EG), hot-dip galvanized (GI), bare steel, and STS 304 specimens. Potentiostatic electrochemical tests revealed that the Zn-flake coating exhibited lower and more stable current densities than EG and GI, indicating a pronounced barrier effect associated with its lamellar structure. Immersion tests (up to 40 days) and cyclic corrosion testing (CCT) further demonstrated superior medium- to long-term corrosion resistance, as evidenced by delayed onset of white and red rust formation and reduced coating degradation. Cross-sectional and EDS analyses also confirmed the structural stability of the coating layers and the suppression of corrosion propagation. These findings suggest that the Zn-flake coating provides an effective approach for enhancing long-term corrosion performance.

Keywords: Zn flake coating, Cyclic salt spray test, Electro-galvanized steel, hot-dip galvanized steel, Corrosion resistance

1. Introduction

Corrosion in structures exposed to high-salinity and high-humidity environments—such as port and offshore facilities, renewable-energy installations, and outdoor industrial plants—has a direct impact on structural integrity and maintenance costs. In particular, carbon-steel bolts and nuts are highly susceptible to accelerated corrosion caused by cyclic wet–dry conditions, salt-water spray, and galvanic interactions. Without appropriate surface protection, such degradation can lead to a loss of clamping force and premature mechanical failure. Hot-dip galvanizing (GI) and electro-galvanizing (EG) have been widely employed to mitigate these issues; however, both processes present inherent limitations, including coating thickness variability, risk of hydrogen embrittlement **[1][2]**, reduced thread precision **[3]**, and insufficient long-term corrosion resistance in harsh environments.

Recently, Zn-flake coatings—composed of zinc flakes dispersed in an inorganic binder—have gained attention as an alternative surface protection technology **[4][5]**. These coatings are applied through a dip–spin process and cured at relatively low temperatures, enabling the formation of uniform films with excellent corrosion resistance even at thin coating thicknesses **[6]**. Moreover, because the process does not induce hydrogen embrittlement, Zn-flake systems are suitable for high-strength fastening components **[7]**. However, most previous studies have relied primarily on salt spray tests (SST) or simple immersion tests, and only limited work has focused on electrochemical characterization of the initial stages of corrosion in these systems.

Potentiostatic electrochemical testing enables the evaluation of metal dissolution behavior and early-stage electrochemical reactivity under a fixed potential, making it a suitable method for distinguishing differences in corrosion mechanisms among Zn-flake coatings, galvanized specimens (EG and GI), and reference materials such as carbon steel and stainless steel. In addition, long-term immersion tests and cyclic corrosion testing are essential for assessing practical corrosion resistance under repeated wet–dry cycles and salt exposure. Cross-sectional analysis combined with energy-dispersive X-ray spectroscopy (EDS) provides critical insights into the microstructural evolution and compositional changes that occur within these coatings over time.

In this study, the corrosion behavior of a dual-layer coating system composed of a high-corrosion-resistant base layer and a Zn-flake topcoat was evaluated in comparison with EG, GI, bare steel, and STS 304 specimens. To this end, potentiostatic testing was conducted to analyze early-stage dissolution behavior, immersion testing was employed to assess medium-term corrosion trends, cyclic corrosion testing was performed to simulate

† Corresponding Author (ORCID: http://orcid.org/0000-0002-6700-6234): Professor, Department of Mechanical System Engineering, Gyeongsang National University, 2 Tongyeonghaean-ro, Tongyeong, 53064, Korea, E-mail: jh.yagi@gnu.ac.kr, Tel: 055-772-9107
1 Professor, Division of Marine Mechatronics, Mokpo National Maritime University, E-mail: k.yeonwon@mmu.ac.kr, Tel: +82-61-240-7237
2 Ph. D., POSSOL INNOTECH, E-mail: ceo@possol.kr

realistic environmental exposure, and cross-sectional and EDS analyses were carried out to examine microstructural and compositional changes. The aim of this work is to systematically elucidate the corrosion mechanisms of the Zn-flake–based dual coating and to verify its performance advantages over conventional galvanizing processes, thereby demonstrating its potential for improving long-term corrosion resistance in marine, plant, and renewable-energy structural applications.

2. Experimental Methods

2.1 Fabrication of the Zn-Flake Coating

The coating specimens used in this study consisted of a dual-layer system comprising a Zn-based corrosion-resistant base layer and a Zn flake topcoat. Prior to coating, the bolt specimens were subjected to alkaline degreasing and ultrasonic cleaning to remove surface contaminants, followed by grit blasting to achieve a surface roughness of approximately Ra ≈ 2–4 μm. The specimens were then pre-dried at ~100 °C to eliminate residual moisture.

The corrosion-resistant base layer was applied using a dip–spin process to ensure uniform deposition and subsequently cured at 200–250 °C, forming a protective layer with a thickness of approximately 10–15 μm. The Zn flake topcoat was applied using the same dip–spin method and baked at 250–300 °C to develop a lamellar upper layer with a thickness of approximately 10–15 μm. The final coating thickness was controlled in the range of 20–30 μm by adjusting the coating and curing steps.

2.2 Cross-Sectional Observation and EDS Analysis

For cross-sectional analysis, the coated bolts were sectioned and mounted in epoxy resin, followed by SiC grinding and fine polishing to prepare metallographic specimens. A scanning electron microscope (SEM) was used to examine the layer thicknesses, interface characteristics, flake orientation, and the presence of pores or microcracks within the Zn-based base coat and the Zn flake topcoat. Elemental distributions of Zn, Al, Zr, and Fe were quantitatively evaluated using EDS to confirm the compositional features of each coating layer.

2.3 Corrosion Resistance Evaluation

2.3.1. Potentiostatic Test

The electrochemical behavior of the Zn-flake coating was evaluated using a potentiostatic test within a three-electrode configuration. The working electrodes consisted of the Zn-flake–coated specimens and comparative materials, including EG, GI, bare steel, and STS304 stainless steel. An Ag/AgCl electrode was used as the reference electrode, and a platinum mesh served as the counter electrode. The electrolyte was a 3.5 wt% NaCl solution. After stabilizing the open-circuit potential for 10 min, a potential step of 0.2 V vs. Ag/AgCl was applied, and the current–time response was recorded for 600 s. The applied potential of +0.2 V vs. Ag/AgCl was selected to impose mild anodic polarization on zinc-based coatings. This potential is sufficiently positive relative to the open-circuit potential to activate anodic dissolution of Zn, while remaining below the range where excessive oxidation or oxygen evolution dominates. Therefore, it enables accelerated yet electrochemically stable conditions suitable for comparing early-stage corrosion kinetics and barrier effects among the Zn-flake coating, EG, GI, and reference materials. The measured current was normalized to the exposed surface area and reported as current density (mA cm^{-2}).

2.3.2 Immersion Test

Immersion testing was conducted by fully submerging the specimens in a 3.5 wt.% NaCl solution for up to 40 days. The samples were retrieved at predetermined intervals (1, 3, 7, 14, 21, and 40 days), rinsed, and examined to document surface changes. The occurrence of white rust, delamination, cracking, and substrate exposure on the Zn–Al flake coating was evaluated and compared with those of the EG and GI specimens.

2.3.3. Cyclic Corrosion Test (CCT)

A cyclic corrosion test was conducted to evaluate the environmental durability of the Zn-flake coating under repeated wet–dry–salt exposure conditions. Each cycle consisted of a salt-spray or salt-immersion stage, a room-temperature holding stage, and a drying stage at 40–60 °C. These cycles were repeated multiple times, and changes in surface appearance, the onset of red rust, and the progression of coating delamination were monitored. This test was designed to simulate the repeated thermal and moisture stresses encountered in actual outdoor environments.

3. Results and Discussion

3.1 Cross-Sectional SEM Analysis

Figure 1(a) shows that the Zn flake coating has a total thickness of approximately 26–28 μm and consists of two distinct regions: a Zn-based corrosion-resistant bottom layer (bright contrast) and an overlying Zn-flake top layer with a darker lamellar structure. The bottom layer adheres closely to the steel substrate and provides the fundamental corrosion protection, whereas the lamellar Zn-flake top layer—formed by overlapping plate-like

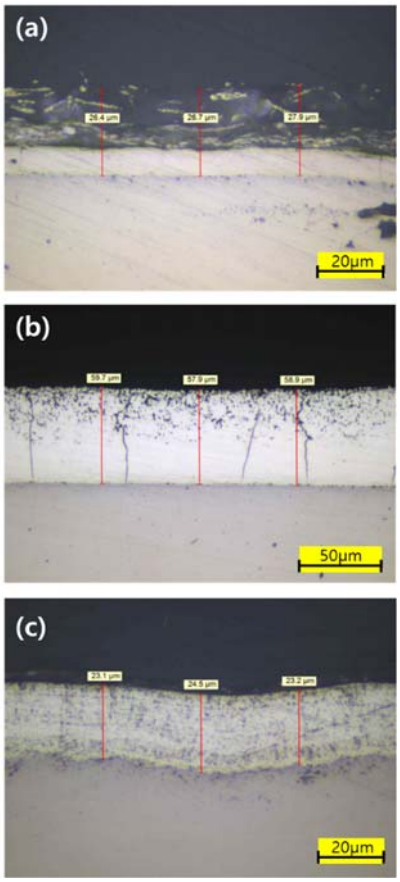

Figure 1: Cross-sectional SEM images of (a) Zn-flake coating, (b) GI coating, and (c) EG coating deposited on carbon steel substrates, respectively

metallic particles—extends the diffusion pathway for water, oxygen, and chloride ions, thereby offering an enhanced barrier effect.

In addition, the upper Zn-flake layer constitutes the first surface exposed to the environment and, upon coating damage or prolonged exposure, the Zn flakes act as a secondary sacrificial anode, providing supplemental protection to the newly exposed areas. This dual protective mechanism is distinct from the behavior of single-layer metallic coatings such as GI or EG and serves as a key factor enabling long-term durability even at relatively thin coating thicknesses.

Figure 1(b) shows that the GI coating exhibits the greatest thickness among the three coating types, measuring approximately 58–60 μm. Its cross-sectional structure consists of the Fe–Zn intermetallic layers typically formed during the hot-dip galvanizing process, overlaid by the η-Zn layer **[8]**. These intermetallic layers are metallurgically bonded to the steel substrate, providing strong adhesion and robust sacrificial protection. Because the GI coating develops a thick and dense metallic layer during solidification, it is generally considered to exhibit superior corrosion resistance and service life **[9]**. The high structural continuity and substantial Zn content allow the coating to suppress corrosion effectively over extended exposure periods.

Figure 1(c) illustrates that the EG coating has a thickness of approximately 23–25 μm and exhibits a fine and uniform single-layer structure. Owing to the characteristics of the electroplating process, Zn is deposited as homogeneous fine grains, resulting in a smoother and more uniform surface compared with GI. Unlike GI, EG coatings do not develop Fe–Zn intermetallic layers, leading to a relatively simple and smooth interface **[10]**. This feature contributes to excellent surface appearance, making EG widely used in applications where aesthetic quality is important, such as automotive and appliance components. However, due to its lower Zn reservoir and thinner coating layer, the long-term sacrificial protection performance of EG is generally considered inferior to that of GI.

The cross-sectional analyses of the three coatings highlight that their distinct manufacturing processes play a decisive role in determining the resulting coating structures. As shown in **Figure 1(a)**, the Zn-flake coating forms a barrier-type architecture in which overlapping metallic flakes create an effective diffusion-resistant pathway even at relatively thin coating thicknesses **[11]**. In contrast, the GI coating achieves superior long-term corrosion resistance due to its substantial thickness and the presence of metallurgically formed Fe–Zn intermetallic layers that enhance sacrificial protection. The EG coating, consisting of a uniform single Zn layer, is well suited for applications prioritizing surface appearance; however, its sacrificial behavior is strongly dependent on coating thickness. These microstructural distinctions are expected to correlate directly with the corrosion resistance trends observed in subsequent electrochemical, immersion, and cyclic corrosion tests.

3.2 EDS Analysis of Coating Composition

Figure 2(a) presents the EDS results obtained from the upper layer of the Zn-flake coating, showing that C (31.93 at.%) and O (65.86 at.%) were present in dominant proportions, while only small amounts of metallic elements such as Fe (0.28 at.%) and Zr (0.35 at.%) were detected. This composition indicates that the analyzed region corresponds not to the Zn flakes themselves but rather to the inorganic–organic hybrid binder matrix that binds the flakes and stabilizes the coating surface. The presence of Zr suggests the incorporation of zirconium-based inorganic additives or Zr-silane surface stabilizers within the Zn-flake

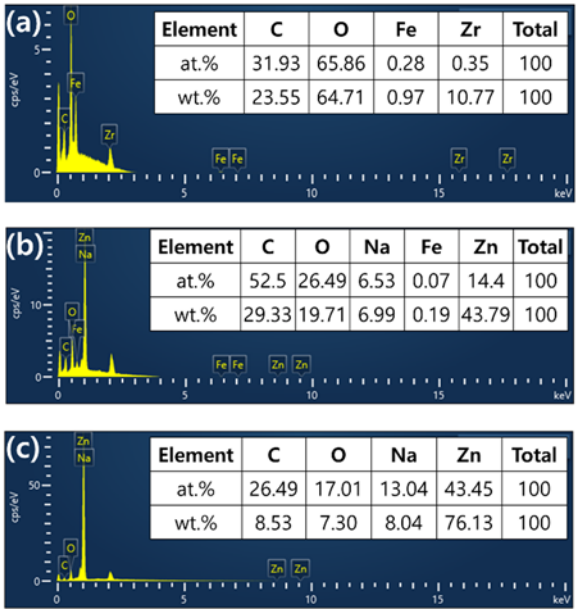

Figure 2: EDS spectra of (a) Zn flake coating, (b) GI coating, and (c) EG coating

formulation, both of which are known to contribute to improved corrosion resistance **[12][13]**. The high fractions of C and O further reflect the structural contribution of the binder matrix, demonstrating that the Zn-flake coating relies on a composite protection mechanism that integrates barrier effects with inorganic electrochemical stability—distinct from conventional metallic Zn coating layers.

Figure 2(b) shows the EDS results for the GI coating, in which Zn was detected at a high level (43.79 wt.%), clearly indicating that the coating is primarily composed of metallic Zn and Fe–Zn intermetallic compounds. The peak observed at approximately ~2 keV corresponds to the Zn L α emission, which is characteristic of Zn-rich coatings analyzed by EDS. This peak originates from the metallic Zn layer and Fe-Zn intermetallic phases formed during the hot-dip galvanizing process. The detection of C (52.5 at.%) and O (26.49 at.%) is attributed either to the presence of a naturally formed ZnO surface film or to surface contamination introduced during sample preparation. The compositional characteristics of GI—namely the presence of a continuous metallic Zn layer—stand in sharp contrast to the Zn-flake coating, where Zn is present in discrete lamellar particles embedded within a binder matrix. This structural distinction aligns with the conventional sacrificial protection mechanism of GI coatings. Consequently, the substantial Zn reservoir and the presence of intermetallic layers suggest that GI provides the strongest long-term sacrificial protection among the three coating systems evaluated.

Figure 2(c) shows that the EG coating contains Zn at 76.13 wt.%, the highest among the three coatings analyzed, confirming that the electro-galvanized layer is composed of a highly uniform, single metallic Zn layer. The detected C and O signals are attributed to surface contamination or the presence of a thin ZnO film, while the detection of Na at 13.04 at.% suggests the possible residue of electrolytic bath components (e.g., salts or additives) used in the electroplating process. These compositional features are consistent with the process characteristics of EG coatings, which are known to form thin, uniform layers with excellent paintability and surface appearance. However, because the Zn layer is continuous but significantly thinner than that of GI, the duration of sacrificial protection is expected to be comparatively shorter.

The EDS results of the three samples clearly demonstrate that their differing corrosion-protection mechanisms originate from fundamental compositional distinctions. Although the Zn-flake coating contains a relatively low overall Zn content due to its flake-laminated architecture, it achieves high corrosion resistance through a combination of barrier effects and electrochemical potential stabilization. In contrast, both GI and EG rely primarily on sacrificial protection, as Zn exists as a continuous metallic layer. Among them, GI provides superior long-term protection owing to its thick Zn reservoir and the presence of Fe–Zn intermetallic layers, whereas EG forms a thin and uniform Zn layer that favors high surface quality but offers a shorter duration of sacrificial action. Overall, although Zn-flake, GI, and EG coatings are all Zn-based corrosion-protection systems, their functional mechanisms differ: Zn-flake acts as a composite barrier coating, GI provides a thick sacrificial Zn layer, and EG forms a uniform thin Zn film.

3.3 Immersion tests

Figure 3 presents the corrosion progression of the coated bolts immersed in a 3.5% NaCl solution for 1–40 days. In the early immersion stage (1–4 days), clear differences in surface appearance were observed depending on the coating type. For conventional Zn-based galvanized coatings, the solution became turbid or slightly brown within a few days, and localized red rust appeared on the specimen surfaces. This behavior is attributed to the rapid dissolution of the Zn layer and the subsequent diffusion of corrosion products into the solution. In contrast, the Zn-flake–coated specimens exhibited almost no color change in the solution and no visible corrosion products on the surface during the same period.

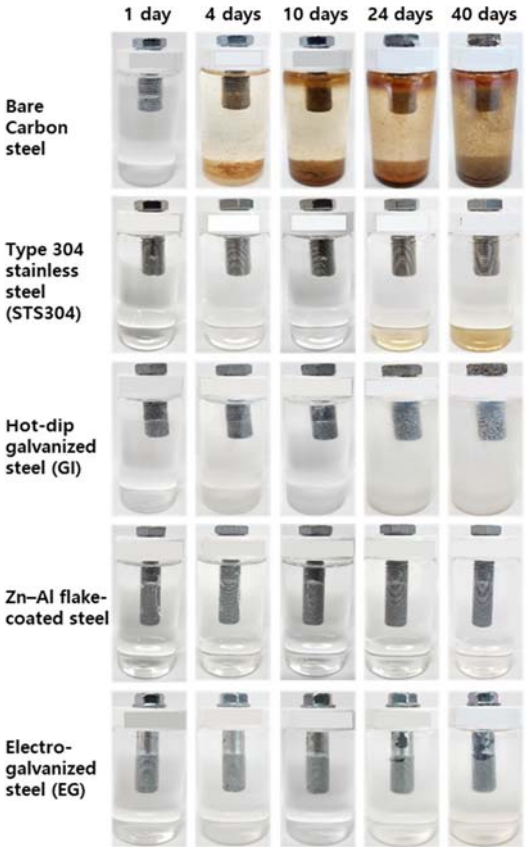

Figure 3: Photographic observations of coated bolts immersed in 3.5% NaCl solution for 1–40 days

During the 10–24day immersion period, the performance differences among the coatings became more pronounced. The GI and EG specimens exhibited progressive spreading of red rust, particularly around the thread regions, and the corrosion-affected areas expanded steadily. The solution also turned yellow–brown, indicating that the Zn sacrificial layer had been depleted and that the underlying Fe substrate had become exposed, leading to the formation of substantial amounts of iron oxides. In contrast, the Zn-flake–coated specimens showed minimal changes in appearance over the same period, and the solution remained clear.

In the later immersion stage (24–40 days), severe corrosion was observed on the conventionally coated specimens, with their surfaces becoming extensively covered by reddish-brown oxides. Corrosion products dispersed throughout the solution, resulting in a marked increase in turbidity. This behavior indicates that the Zn metallic layers had been completely consumed, allowing continuous corrosion of the exposed steel substrate. In contrast, the Zn-flake–coated specimens retained an appearance nearly identical to their initial state, and the solution remained clear even after long-term exposure. This superior stability is attributed to the combined action of the lamellar Zn-flake top layer, which

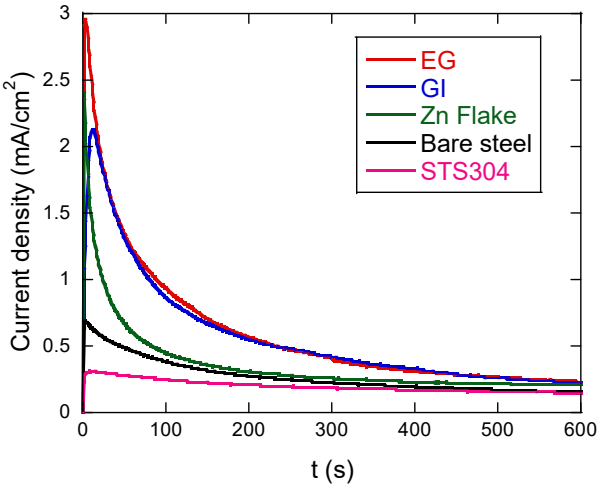

Figure 4: Potentiostatic current–time curves at 0.2 V vs. Ag/AgCl for Zn flake, EG, GI, bare steel, and STS304 specimens

provides a strong barrier effect, and the underlying Zn-based corrosion-resistant layer, which further suppresses electrolyte penetration and inhibits electrochemical reactions at the steel substrate.

3.4 Potentiostatic Tests

In **Figure 4**, upon the application of 0.2 V, all specimens exhibited a distinct initial current peak followed by a time-dependent decay toward a quasi-steady state. This behavior indicates rapid double-layer charging and initial active dissolution, after which the formation of oxides or corrosion products characteristic of each material partially suppressed the electrochemical reactions **[14]**. The overall decreasing trends reflect the initial reactivity of the materials, showing the order EG > GI > Zn-flake > bare steel > STS304, each exhibiting a different slope and final stabilized current level.

The EG and GI specimens displayed the highest initial current densities, consistent with the rapid anodic dissolution of metallic Zn immediately after the potential step. EG showed the most pronounced response because its surface consists almost entirely of a pure Zn layer, whereas GI—although containing Fe–Zn intermetallic phases—still maintained high anodic activity. For both coatings, the current quickly decreased as corrosion products such as $Zn(OH)_2$ and ZnO formed on the surface, reducing active dissolution and facilitating stabilization.

The Zn-flake–coated specimens exhibited a lower initial current and a more gradual decay compared with EG and GI. This behavior reflects the barrier function of the lamellar Zn-flake architecture combined with the binder matrix, which effectively restricts electrolyte diffusion and electron transfer. As a result, the

Zn-flake coating maintained relatively low and stable current densities over extended periods, indicating a controlled sacrificial dissolution process.

Bare steel showed intermediate current levels associated with initial active dissolution, followed by a gradual decrease as $Fe(OH)_3$ and other iron oxyhydroxides formed, producing a partial and temporary passive layer. Although its stabilized current was lower than that of Zn-based coatings, this does not imply superior corrosion resistance because Fe corrosion progresses even under lower anodic current conditions. In contrast, STS304 consistently exhibited the lowest current density among all specimens. The Cr-rich passive film remained stable even at 0.2 V, sustaining a persistent passive state throughout the test. No abrupt current spikes or unstable behavior were observed, indicating an absence of pitting initiation within the test duration.

4. Conclusion

In this study, the corrosion behavior of steel specimens coated with a high-corrosion-resistant Zn-flake system was evaluated through potentiostatic testing, immersion testing, and cyclic corrosion testing (CCT), and the results were compared with those of EG, GI, bare steel, and STS 304. The potentiostatic test revealed that the Zn-flake coating exhibited significantly lower and more stable current densities than EG and GI, reflecting the barrier effect of its lamellar flake structure and the controlled sacrificial dissolution rate. Bare steel showed partial passivation after initial active dissolution, whereas STS304 maintained a stable passive state throughout the experiment.

The immersion test (up to 40 days) further confirmed that the Zn-flake coating demonstrated superior medium-term corrosion resistance, showing delayed onset of white and red rust and reduced surface degradation compared with EG and GI. Similarly, under cyclic wet–dry and salt-exposure conditions in the CCT, the Zn-flake coating exhibited delayed coating degradation and rust formation, indicating improved environmental durability relative to conventional galvanized layers.

Cross-sectional observations and EDS analyses revealed that the Zn-flake coating maintained a relatively stable lamellar structure and compositional distribution even after corrosion exposure, and that corrosion propagation was effectively suppressed. Collectively, these results demonstrate that high-corrosion-resistant Zn-flake coatings offer a promising alternative for enhancing the long-term corrosion durability of steel fasteners used in harsh outdoor and marine environments.

Author Contributions

Conceptualization, K. Lee and J. Yang; Methodology, J. Yang; Investigation, Y. Kim, K. Lee; Resources, K. Lee and J. Yang; Data Curation Y. Kim; Writing-Original Draft Preparation, Y. Kim; Writing-Review & Editing, Y. Kim and J. Yang; Visualization, Y. Kim; Supervision, J. Yang; Project Administration, J. Yang.

References

[1] A. Milone, P. Foti, L. M. Viespoli, D. Wan, F. Mutignani, R. Landolfo, and F. Berto, “Influence of hot-dip galvanization on the fatigue performance of high-strength bolted connections,” Engineering Structures, vol. 299, 117136, 2024.

[2] P. Shreyas, B. Panda, and A. D. Vishwanatha, “Embrittlement of hot-dip galvanized steel: A review,” AIP Conference Proceedings, vol. 2317, no. 1, art. no. 020038, 2021.

[3] Z. Yu, J. Hu, and H. Meng, “A review of recent developments in coating systems for hot-dip galvanized steel,” Frontiers in Materials, vol. 7, art. no. 74, 2020.

[4] C. Qi, K. Dam-Johansen, C. E. Weinell, H. Bi, and H. Wu, “Enhanced anticorrosion performance of zinc-rich epoxy coatings modified with stainless steel flakes,” Progress in Organic Coatings, vol. 163, art. no. 106616, 2022.

[5] N. Hoang, *et al.*, “Flake ZnAl alloy as an effective pigment in silicate coatings for the corrosion protection of steel,” Coatings, vol. 12, no. 8, art. no. 1046, 2022.

[6] F. Feldmann, *et al.*, “Characterisation of the galvanic protection of zinc flake coating by spectroelectrochemistry and industrial testing,” Materials and Corrosion, vol. 74, no. 8, pp. 1148-1158, 2023.

[7] M. Kumar, E. Persson, I. Sherrington, and S. Glavatskih, “Changes in friction of zinc flake-coated threaded fasteners due to humidity, temperature and storage duration,” Tribology International, vol. 170, art. no. 107498, 2022.

[8] T. Pinger, *et al.*, “Abrasive wear behavior of batch hot-dip galvanized coatings,” Materials, vol. 17, no. 7, art. no. 1547, 2024.

[9] Z. Li, *et al.*, “A review of physical properties of hot-dip galvanized coating layer by layer and their respective electrochemical corrosion behavior,” Anti-Corrosion Methods and Materials, vol. 71, no. 5, pp. 580-589, 2024.

[10] J. Zhou, *et al.*, “Effect of the electrogalvanized and galvannealed Zn coatings on the liquid metal embrittlement

susceptibility of high Si and Mn advanced high-strength steel," Coatings, vol. 15, no. 1, art. no. 28, 2025.

[11] J. Zhang, *et al.*, "Flake-like ZnAl alloy powder modified waterborne epoxy coatings with enhanced corrosion resistance," Progress in Organic Coatings, vol. 175, art. no. 107367, 2023.

[12] N. Hoang, *et al.*, "Corrosion protection of carbon steel using a combination of Zr conversion coating and subsequent zinc-rich silicate coating with a flake ZnAl alloy," Arabian Journal of Chemistry, vol. 15, no. 6, art. no. 103815, 2022.

[13] H. R. Asemani, *et al.*, "Effect of zirconium conversion coating: Adhesion and anti-corrosion properties of epoxy organic coating containing zinc aluminum polyphosphate (ZAPP) pigment on carbon mild steel," Progress in Organic Coatings, vol. 94, pp. 18-27, 2016.

[14] Y. Meng, *et al.*, "Initial formation of corrosion products on pure zinc in saline solution," Bioactive Materials, vol. 4, pp. 87–96, 2019.

[15] M. Bockelmann, *et al.*, "Passivation of zinc anodes in alkaline electrolyte: Part I. Determination of the starting point of passive film formation," Journal of The Electrochemical Society, vol. 165, no. 13, pp. A3048–A3055, 2018.